UCRL-16637

University of California

Ernest O. Lawrence Radiation Laboratory

THE 7.7-METER BENT-CRYSTAL SPECTROMETER
AT THE 184-INCH CYCLOTRON

TWO-WEEK LOAN COPY

This is a Library Circulating Copy which may be borrowed for two weeks. For a personal retention copy, call Tech. Info. Division, Ext. 5545

Berkeley, California

DISCLAIMER

This document was prepared as an account of work sponsored by the United States Government. While this document is believed to contain correct information, neither the United States Government nor any agency thereof, nor the Regents of the University of California, nor any of their employees, makes any warranty, express or implied, or assumes any legal responsibility for the accuracy, completeness, or usefulness of any information, apparatus, product, or process disclosed, or represents that its use would not infringe privately owned rights. Reference herein to any specific commercial product, process, or service by its trade name, trademark, manufacturer, or otherwise, does not necessarily constitute or imply its endorsement, recommendation, or favoring by the United States Government or any agency thereof, or the Regents of the University of California. The views and opinions of authors expressed herein do not necessarily state or reflect those of the United States Government or any agency thereof or the Regents of the University of California.

Submitted to
Rev. of Scientific Instruments

UCRL-16637

UNIVERSITY OF CALIFORNIA

Lawrence Radiation Laboratory
Berkeley, California

AEC Contract No. W-7405-eng-48

THE 7.7-METER BENT-CRYSTAL SPECTROMETER AT THE 184-INCH CYCLOTRON

Kenneth M. Crowe and Robert E. Shafer

April 19, 1966

The 7.7-Meter Bent-Crystal Spectrometer at the 184-Inch Cyclotron*

Kenneth M. Crowe and Robert E. Shafer†

Lawrence Radiation Laboratory
University of California
Berkeley, California

April 19, 1966

ABSTRACT

We describe the design, operation, and calibration of a 7.7-m DuMond-geometry bent-crystal spectrometer, constructed at the 184-Inch Cyclotron for the study of mesonic x rays. The application of crystal-diffraction techniques to mesonic x-ray measurements is briefly discussed.

I. INTRODUCTION

Crystal-diffraction spectrometry has been recognized for many years as a precise method of measuring the energies (wavelengths, actually) of nuclear gamma and electronic x-rays. The development of DuMond-geometry bent-crystal spectrometers[1-3] with their relatively high efficiency has made possible the application of crystal-diffraction techniques to previously inaccessible areas of research. In this paper we describe a DuMond-geometry spectrometer built specifically for mesonic x-ray studies at the 184-Inch Cyclotron.

In Section II we describe the design and construction of the spectrometer, and in Section III its operation and calibration. In Section IV application of crystal-diffraction techniques to mesonic x-ray measurements is discussed briefly.

II. DESIGN AND CONSTRUCTION OF THE SPECTROMETER

The instrument described here is a line-source transmission spectrometer, often referred to as the DuMond or Monochromator arrangement. The general design of these instruments as well as other crystal spectrometers is described in several excellent review articles.[4-8] The focal geometry of the instrument described here is illustrated in Fig. 1. Its mechanical construction resembles that of several other monochromators, including one of comparable (7.7 m) focal length[9] and several with shorter (usually 2 m) focal lengths.[10] In this instrument, as in the others, the source is at a stationary focus of the bent crystal, and the Bragg conditions are satisfied by rotating the bent crystal about a stationary vertical axis. A sine-screw mechanism is used to rotate the crystal

and measure the Bragg angles with respect to the spectrometer foundation. The collimator-detector assembly is independently rotatable about the bent-crystal axis and is positioned to selectively transmit the diffracted x-rays. Table I summarizes the important parameters of the instrument.

Overall top and side views of the spectrometer are illustrated in Figs. 2 and 3. The foundation is a 30-ton concrete block cast in a shock-absorbent mounting. A surplus Navy gun mount is used to support and rotate the entire detector-collimator assembly (including about 5 tons of shielding), which is balanced by a counterweight. As moments about the gun mount are approximately cancelled, rotation of this assembly does not affect the alignment of the spectrometer.

The crystal pivot assembly is mounted rigidly to the concrete foundation through a hole in the center of the gun mount. This assembly is illustrated in Fig. 4. The central bearings are special class-9 Fafnir ball bearings with a maximum radial runout of 50 μin. and ball sphericity within 5 μin. The two bearings are preloaded against each other with 1000 lb force to remove axial and radial play. The final machining of the crystal pivot table was done using these bearings to define the axis of rotation, hence minimizing table runout. The axial thrust is carried by the outer race of the lower bearings.

Above the bearings in Fig. 4 is the 23-in. diam engraved horizontal circle[11] used for positioning the collimator assembly with respect to the crystal orientation. Microscopes mounted on the gun mount are used to interpolate between the 0.1-deg inscriptions to a precision of ±10 seconds [the collimator resolution (FWHM) is about 900 sec]. The inscriptions are accurate within ± 0.5 sec. The horizontal circle may also be

used to measure the crystal orientation with respect to the spectrometer foundation by means of another set of microscopes. This allows a direct check of the sine-screw mechanism, which is the primary means of measuring Bragg angles.

The sine-screw mechanism is illustrated in Fig. 5. The 1.25-in. diam stress-proof-steel lead screw is supported by class-9 Fafnir ball bearings, the axial thrust being borne by the two angular-contact preloaded bearings at the crank end. The bronze split-nut is attached to a full-gimbal yoke which makes a 3-point contact with the sliding block. The motion of the sliding block is collimated by a guide plate. The endplate of the sliding block pushes against a 1.5-in.-diam precision steel ball mounted in the pivot arm. A constant azimuthal torque is applied directly to the pivot arm by a suspended-weight arrangement, the torque being counterbalanced by an axial thrust in the sine screw. The entire mechanism is enclosed in a dustproof Lucite case.

The lead screw and the split nut were lapped together after the machining process, and a linearity check was made by comparison with a precision-engraved steel rule. The mean pitch was determined to be 32.0019 turns/in., and the deviations from linearity were found to be less than ±37 μin., as illustrated in Fig. 6. This is about the limit of precision obtainable by comparison with an engraved rule. A correction cam is provided for correcting nonlinearities, but the precision required for mesonic x-ray measurements has not yet warranted its use. Synchronous axial motion of the lead screw due to axial runout in the preloaded bearings was determined to be 30±5 μin. peak-to-peak, using air-gage techniques. As all the above linearity measurements were taken an integral number of turns apart, they are not correlated with the axial motion. The length of the pivot arm is 22.0000±0.0002 in. (we refer to this as the low-energy arm), and the useable region of the lead screw is about 90 turns each side

of center, allowing measurement of Bragg angles up to 27,000 sec each side [this corresponds to a lower limit of 40 keV, first order, both sides, for quartz (310) diffraction]. The total mechanical error, including both systematic (nonlinearity) and statistical (nonrepeatability) contributions, is expected to be within ± 46 μin., which corresponds to ± 0.43 sec of arc [these errors correspond to ±0.005 xu for diffraction from quartz (310) planes]. Two other available pivot arms, being two and five times the length of the low-energy arm respectively, can be installed by moving the sine-screw mechanism. These arms allow higher angular precision, but limit correspondingly the range of measurable angles.

The crystal-clamp blocks (the method of imprisonment is used here) were cast from type 420 stainless steel, annealed, and then ground on a machine specifically built for this application.[12] Both the convex and concave form blocks were then lapped against cast-iron blocks ground to the same radius of curvature. The convex form block has an aperture of 13.7 by 13.7 cm^2 with a single 1.6-cm-wide rib across the center, leaving about 160 cm^2 open area.

The quartz plate, supplied by Hilger and Watts Ltd. to specifications written by J. W. M. DuMond,[13] was cut to 20- by 20- by 0.6 cm^3 with the (310) planes normal to the two faces and two edges. The plate, etched with HF to reduce the possibility of breakage, was clamped between the form blocks with a 0.2- cm-thick neoprene gasket on the convex side. The first constructive-interference fringe between the steel rib and the quartz plate was about 1 cm in from each edge of the aperture. Figure 7 illustrates the imprisoned crystal.

A cross section of the collimator is shown in Fig. 8. It is of the flat-plate, tapered-gap design, the plates being 1 mm thick and the

gaps approximately 3 mm wide (we refer to this as the low-energy collimator). The 44 lead-alloy plates were manufactured from low-background lead supplied by the St. Joseph Mines.[14] The collimator has an aperture of about 18 by 18 cm^2 and is 94 cm long. Construction included stretching the plates lengthwise, fastening them to the upper and lower guide plates with a room-temperature-cure epoxy cement, and finally stretching them vertically as indicated in the Figure. The collimator, designed for use at low energies (Bragg angles $\geqslant 1$ deg), has an estimated transmission efficiency of 0.65 based on the performance of an earlier design (this earlier version has a 1-to-1 plate-to-gap ratio and is reserved for high-energy measurements). The measured resolution of the low-energy collimator is about 900 sec of arc for 84 keV γ-rays.

The detector is a 17-by 17-by 0.63 cm^3 packaged NaI(Tℓ)[15] crystal viewed on one face by nine RCA 6810's through a 2-in.-long Lucite light pipe. The system was balanced for uniform pulse-height output over the entire NaI(Tℓ) surface by using a radioactive source and varying the anode voltages individually. The pulse-height resolution corresponds approximately to 0.75 photoelectrons per keV of x-ray energy. Its total efficiency is greater than 90% for x-rays below 120 keV.

Unlike many bent-crystal spectrometers, no provision has been made for automatic scanning of spectra by synchronously rotating the crystal and collimator with the required 1:2 ratio of angular velocities. Due to the very low counting rates encountered in mesonic x-ray diffraction, the rotation is accomplished manually at periodic intervals, by using the cranks illustrated in Fig. 2. The relative alignment of the crystal and collimator is checked by using the graduated circle described earlier.

As the spectrometer is situated near the 184-Inch Cyclotron, the background radiation, due mainly to neutrons, necessitates a considerable amount of shielding around the NaI detector and collimator. The system is almost completely surrounded by a minimum of 4 in. of lead. Outside the lead is about 12 in. of paraffin and boric acid, and inside the lead a 1/4-in. layer of boron carbide. The total weight of this shielding is about 5 tons, and is counterbalanced as shown in Figs. 2 and 3.

In addition to this shielding, the bent-crystal "cave" is surrounded by concrete (minimum thickness about four feet) and by battleship armor plate (thickness about one foot). None of the weight of this additional shielding rests upon the shock-absorbent foundation.

In the pulse-height region 50 keV < E < 200 keV, less than 5% of the NaI background can be correlated with the cyclotron beam. The background, about 0.09 counts/keV-sec, is due almost entirely to natural radioactivity inside the shielding.

III. PERFORMANCE AND CALIBRATION

The quality of the bent crystal was checked by performing a Hartmann test[16] with a 0.5 Curie Au^{198} source. The 0.25-mm-diam gold wire, irradiated at the Livermore pool type reactor, was held taut and vertical by a 500-g weight. The test indicated that the focusing properties were uniform, even near the edges, and hence that the entire aperture could be used. The optimum focal-circle-diameter was determined to be about 764 cm, 6 cm shorter than expected (the first crystal installed in the 7.7-m Argonne spectrometer showed a similar deviation).

Diffraction from the entire crystal yielded an optimum resolution of 17 sec of arc (FWHM) as shown in Fig. 9. As a comparison, a smaller

6-mm quartz crystal bent by Argonne to 7.7 meters showed a resolution of 13 sec.[9] A thinner crystal would be expected to show better resolution, but with a loss of reflectivity. As 17 sec corresponds to an effective source width of 0.63 mm, the contribution from the finite diameter of the gold wire is small. Least-squares analysis of the diffraction peak shows that it is reasonably symmetric and may adequately be represented by a Gaussian distribution. (It is important to note that any instrumental asymmetry will occur in both the right and left diffraction peaks with the same parity, so that if the Bragg angle is found by measuring the angular separation of these peaks, any effect of the asymmetry will be completely cancelled.)

The energy resolution (FWHM) is then (keV units):

$E = 10$

$$\Delta E = 1.6 \times 10^{-5} E^2$$

$\Delta E = 10^{-3} = 1\,eV$

7.2 eV @ 21 keV (1)

for first-order diffraction. The mechanical errors mentioned in Section II presently limit the precision to about 2.5% of the resolution (note that by convention, resolution is measured in FWHM, and precision in standard deviations).

The total efficiency may be calculated from geometrical factors, absorption coefficients of air and quartz, and the crystal reflectivity. The mechanical solid angle subtended by the crystal is $4\pi \times 2.2 \times 10^{-5}$ sr, and the estimated transmission efficiency of the collimator is 0.65.

When x rays are transmitted through a crystal in such a way that the Bragg conditions are satisfied, a fraction of the total transmitted intensity, defined here as the reflectivity, is expected to be in the diffracted beam. The integrated reflectivity is the reflectivity integrated over the diffraction peak. Secondary extinction refers to the removal of intensity from either the incident or diffracted beams by (multiple) diffraction in

the crystal (i.e., the maximum reflectivity is 0.5). This apparent saturation of the reflectivity can affect the shape of the diffraction peak. Primary extinction, a coherent process taking place in the small "perfect" mosaic "blocks" within the macroscopic crystal, has been shown by Lind et al.[17] to be negligible in bent quartz crystals for the wavelength region of interest here, and will not be discussed further. The reflectivity of the quartz crystal used here is expected to exhibit the $1/E^2$ energy dependence of mosaic crystals, modified only by the secondary extinction process. A more complete discussion of the diffraction process in perfect and mosaic crystals is presented by Lind et al.[17] and Zachariasen.[18]

The reflectivity of the 6-mm-thick bent quartz crystal may be derived from the integrated reflectivity measured for a 1-mm-thick bent quartz crystal by Lind et al.[17] The calculated reflectivity is illustrated in Fig. 10. The effect of secondary extinction is observable below 100 keV. The total efficiency, based on reflectivity, absorption, and geometrical factors, is shown in Fig. 11. As can be seen, below 50 keV the efficiency drops off rapidly due to absorption of the x rays in air and the quartz crystal. The maximum efficiency is expected to be about 2.5×10^{-6} at an energy of 50 keV.

The remainder of the performance tests, and the final calibration, were carried out with a 1-mm-diam, 10-cm-high Tm^{170} source in a quartz tube. The 0.5-Curie source was in the form Tm_2O_3. The radiations of interest are the nuclear gamma ray and the $K\alpha_1$ x-ray of Yb^{170}:

Transition	Wavelength (xu)	Energy (keV)
84-keV γ ray	146.835 ± 0.005	84.261 ± 0.003[19]
$K\alpha_1$ x ray	236.165 ± 0.003[20]	52.389 ± 0.001

The wavelength-energy conversion constant used throughout this paper is 12372.42 xu-keV ± 15 ppm.[20] It is worthwhile to mention that the spectrometer resolution for the x ray, which has a natural width of 35 eV, is 45 eV; hence the observed lineshape is distinctly different for the two radiations, the x ray showing the "skirt" typical of resonances.

The most precise method of measuring Bragg angles is to measure the angular separation of the right and left diffraction peaks, in this case first-order. It is of considerable importance to check the repeatability of the instrument in order to understand as well as possible the sources of error.

The sine-screw mechanism measures the sine of the angle between the diffraction peak and a point on the lead screw defined mechanically to be the "mechanical center." As the angular separation between the right and left first-order diffraction peaks is $2\theta_B$, the sine-screw mechanism measures $2 \sin\theta_B \cos\delta$, as shown in Fig. 12. The angle δ is variable from approximately -4000 to +4000 sec by moving the source. Normal operation of the spectrometer is performed with $\delta \leq 100$ sec so that the $\cos\delta$ factor may be set equal to 1. Figure 13 shows measured values of $\sin\theta_B \cos\delta$, using the 84-keV γ ray, plotted vs the midpoint (which is defined in Fig. 12). The smooth curve is a best fit of the form $A \cos\delta$, the expected shape.

The thermal-expansion coefficient of the quartz (310) planes is 15 ppm/°C.[21] The only other thermal-expansion correction, due to differential expansion of mechanical parts, is estimated to be less than ± 5 ppm/°C effective contribution. No such anomalous temperature dependence has been observed. By convention, all measurements are corrected to 18°C.

Because of the particular application for which this instrument was built, long-term stability is important. In Fig. 13, seven of the points were measured in December 1964 and three in March 1965 (the most recent mesonic x-ray experiment took place in this interval). The observed shift was less than ± 0.002 xu.

The error flags in Fig. 13, determined purely on the basis of external consistency (i.e., from residuals), represent a wavelength deviation of ± 0.002 xu. In each case the sample mean of the diffraction peaks was determined by χ^2 analysis, and the purely statistical fluctuations were estimated to be less than ±0.001 xu. Although the observed wavelength precision is somewhat better than the ± 0.005 xu predicted by mechanical considerations, it should be realized that this test only compares the relative linearity of two regions of the sine screw, each about 30 turns wide.

The possibility that small-angle Compton scattering of x-rays in a thick source could produce a noticeable effect on the position or shape of the diffraction peak was considered. An attempt to observe such an effect was made by placing 1-in.-thick aluminum filter directly in front of the source. No effect (other than attenuation) was observed within the limits of precision of the instrument.

The calibration of the instrument by using the nuclear gamma and the electronic x-ray yielded the following data:

Transition	$\sin\theta_B$	d_{18} spacing
84-keV γ-ray	0.0623509	1177.49 ± 0.06 xu
52-keV x-ray	0.1002770	1177.56 ± 0.03 xu

The entire calibration error for each transition is contained in the error on the respective d spacing. The deviation between the two d

spacings is due possibly to either a nonlinearity in the sine-screw mechanism or a slight shift in the value quoted for the wavelength of one of the calibration lines.

IV. APPLICATION TO MESONIC X-RAY STUDIES

Most of the published studies of pionic and muonic x-rays have been performed with scintillation and proportional counters, sometimes in conjunction with absorption-edge filters. Several review articles outline these studies.[22-26] Recent application of solid-state detectors to this field has yielded absolute measurements with considerably higher precision.[27, 28] Application of crystal-diffraction techniques to mesonic x-ray studies thus far has been performed only with the instrument described in this paper,[29, 30] although plans for similar experiments at other facilities are in progress.[31]

The energy region in which bent-crystal spectroscopy can presently be applied to mesonic x-rays is limited to the interval $20\,\text{keV} \leq E \leq 200$ keV owing to the energy dependence of the efficiency of these instruments (see for example Fig. 11). This is in contrast to scintillation and semiconductor detectors, which can analyze the entire spectrum above 20 keV. Use of other diffraction crystals can extend the useable region of crystal spectrometers above 200 keV, however, and the superior resolution and precision obtainable by crystal diffraction in the low-energy region make this technique a complementary method of studying mesonic x rays. At 50 keV, for example, where the efficiency of the instrument described here reaches a maximum of about 2.5×10^{-6}, the instrumental resolution is about 40 eV (FWHM) and the obtainable precision about ± 1 eV (see Table I). Two pionic x rays in the 50- to 100-keV region have been measured to

±9 eV precision.[30]

Optimum source strengths for bent-crystal spectroscopy (using the DuMond geometry) are usually in the 0.1 to 10 Curie range, depending on the spectrometer efficiency. This is in contrast to the obtainable "source" strengths for mesonic x-rays, which at present do not exceed a few microcuries. In particular, for the pionic x-ray studies at Berkeley, the maximum stopping pion rate is of the order of 4×10^5/sec (with a 60% macroscopic duty cycle), and the yield of pionic x rays is somewhat lower. The maximum obtainable density of stopping pions is about 800 pions/g sec for most target materials, the corresponding specific x-ray activity being of the order of 10^{-2} μCurie/g. Muonic x-ray yields at the 184-Inch Cyclotron are about an order of magnitude lower.

Mesonic x-ray "sources" are not very flexible in their design. The overall dimensions of the "source" depend on the momentum spread and phase space of the meson beam, as well as range straggling. The "source" must be stationary as are meson-producing accelerators. The duty cycle of the accelerator should also be considered. In brief, the crystal spectrometer should be designed to complement the mesonic x-ray "source".

As the focal length f of the spectrometer determines the focal volume ($\propto f^3$), the crystal thickness and hence the reflectivity (approximately $\propto f$), and the solid angle subtended by the crystal ($\propto f^{-2}$), the optimum focal length occurs approximately where two of the linear dimensions of the x-ray "source" (which may include only a small fraction of the total stopping meson beam) are limited by factors other than focusing aberrations. In the DuMond arrangement these factors include the dimensions of the

volume of stopping mesons, and the x-ray attenuation length in the "source" material. In the Cauchois geometry, these factors are determined by the characteristics of the x-ray detector.

Typically the efficiency of a DuMond-geometry instrument is about a factor of 200 larger than the efficiency of a Cauchois-geometry instrument with the same bent crystal. This gain is to a large extent cancelled by the limitation that only a small fraction of the meson beam can be stopped within the focal volume of a reasonable-focal-length DuMond-geometry instrument (the fraction is about 1% for the instrument described here). Although a Cauchois-geometry instrument exhibits an efficiency comparable to flat-crystal instruments, a very considerable gain is realized since the x-ray detector is located at the crystal focus and is therefore relatively small. This leads to a considerable reduction in the background counting rate.

The experimental arrangement used with the 7.7-m bent crystal monochromator is illustrated in Fig. 14. The stopping pion is identified by a scintillation-counter telescope (Fig. 15). Diffracted pionic x rays are detected by the NaI(Tℓ) scintillator, which is in fast coincidence with the scintillation-counter telescope. Pulse-height analysis alone on the NaI(Tℓ) signal reduces the background typically to about 3 counts/sec in the pulse-height interval of interest, and the additional coincidence requirement (timing resolution ~ 10 nsec FWHM) reduces the background further to about 3 counts/hour. Observed diffracted pionic x-ray rates are of the order of 2 to 3 events/hour. Typical diffraction peaks are illustrated in Fig. 16.

As with any long-term measurement by crystal diffraction, stability of alignment, as well as temperature, is important. As illustrated in Fig. 14, an autocollimator, whose base is a large concrete block grouted to the floor of the experimental area, is used in conjunction with an optical-alignment target mounted on the convex bent-crystal form block to define a line of sight. In addition, the form block with a front-surface mirror attachment can be rotated into autocollimation as an additional alignment check. Such checks are performed at regular intervals throughout the experiment. The precision obtainable with the present optical alignment system is marginal, however, and for this reason any improvement in experimental precision should be accompanied by an improved method of monitoring the alignment.

ACKNOWLEDGMENTS

We would like to express our deep appreciation to Professor J. W. M. DuMond for his continued interest and participation in the development of this facility. Professor DuMond has been a consultant on this project since its inception ten years ago.

We appreciate the efforts of the many engineers and machinists who have contributed to the successful construction of the spectrometer. Special tribute is due Ralph Peters and Dwight Vorkoeper, who ingeniously and patiently designed the instrument. Albert Kleid contributed significantly to the precision alignment of the spectrometer.

We wish to thank Dr. Walter John for successfully etching and bending the 6-mm quartz crystal.

We are very grateful to Dr. Alan Astbury, Dr. Jules Deutsch, and Dr. Richard Taylor, who jointly are responsible in large part for the initial operation of the instrument.

The support and encouragement received from Professors Robert Thornton and Edwin McMillan, as well as the cooperation of James T. Vale and the Cyclotron crew, is gratefully acknowledged.

FOOTNOTES AND REFERENCES

*This work was performed under the auspices of the U. S. Atomic Energy Commission. This report is derived from the thesis presented by one of the authors (R. E. S.) in partial fulfillment of the requirements for the degree of Ph. D. in Physics.

†Now at the Laboratory for Nuclear Science, Massachusetts Institute of Technology, Cambridge, Mass.

1. J. W. M. DuMond and H. A. Kirkpatrick, Rev. Sci. Instr. 1, 88 (1930).
2. J. W. M. DuMond, Rev. Sci. Instr. 18, 626 (1947).
3. E. J. Seppi, H. Hendrickson, F. Boehm, and J. W. M. DuMond, Nucl. Instr. Methods 16, 17 (1962).
4. J. W. M. DuMond, in Beta and Gamma Ray Spectroscopy, edited by K. Siegbahn (North Holland Publishing Co., Amsterdam, 1955), p. 100.
5. J. W. M. DuMond, Ergeb. Exakt. Naturw. 28, 232 (1955).
6. J. W. M. DuMond, Ann. Rev. Nucl. Sci. 8, 163 (1958).
7. G. A. Bartholomew, J. W. Knowles, and G. E. Lee-Whitting, Rept. Progr. Phys. 23, 453 (1960).
8. J. W. Knowles, in Beta and Gamma Ray Spectroscopy, edited by K. Siegbahn (North Holland Publishing Co., Amsterdam, 1965), p. 203.
9. D. Rose, H. Ostrander, and B. Hamermesh, Rev. Sci. Instr. 28, 233 (1957). For a more complete description see Argonne National Laboratory Report ANL 5642, December 1956. (unpublished).
10. Several research groups have constructed 2-m instruments following the design of Seppi et al. in Ref. 3.

11. Engraved by W. and L. E. Gurley, Troy, New York.

12. H. Ostrander, American Machinist 100, 118 (July 2, 1965). We are grateful to H. Ostrander and Argonne National Laboratory for grinding and lapping the form blocks.

13. The specifications for the quartz plate are outlined in Ref. 9.

14. The Pb-alloy plates were fabricated by the National Lead Co., Granite City, Illinois.

15. The packaged NaI(Tℓ) scintillator was built to our specifications by Harshaw Chemical Co.

16. An excellent description of the Hartmann test is given in Ref. 5, p. 267 to 268.

17. D. A. Lind, W. J. West, and J. W. M. DuMond, Phys. Rev. 77, 475 (1950).

18. W. H. Zachariasen, Theory of X-Ray Diffraction in Crystals (John Wiley and Sons, Inc., New York, 1945).

19. I. Marklund and B. Lindstrom [Nucl. Phys. 40, 329 (1963)] measure an energy of 84.260±0.004 keV for this transition (their quoted value has been modified slightly from 84.262±0.004 keV due to a reevaluation of the wavelength of their calibration line).[20] F. Boehm and C. Gunther (private communication, 1965) have measured this line by direct comparison with the K_α x rays,[20] obtaining the value 84.261± 0.003 keV.

20. J. A. Bearden, X-Ray Wavelengths, U. S. A. E. C. Report NYO-10586, 1964, unpublished. This is a 530-page compilation of measurements of the wavelengths of more than 25 000 electronic x rays. We re-express this author's errors in standard deviations in this paper.

21. B. B. Watson, W. J. West, D. A. Lind, and J. W. M. DuMond, Phys. Rev. 75, 505 (1949).

22. S. DeBenedetti, Nuovo Cimento (10) 4, 1209 (1956).

23. M. B. Stearns, Progr. Nucl. Phys. 6, 108 (1957).

24. D. West, Rept. Progr. Phys. 21, 271 (1958).

25. J. Rainwater, Ann. Rev. Nucl. Sci. 7, 1 (1957). See p. 17 et seq.

26. G. Feinberg and L. M. Lederman, Ann. Rev. Nucl. Sci. 13, 431 (1963). See sections II-D and V-A.

27. D. A. Jenkins and K. M. Crowe, Phys. Rev. Letters 16, 637 (1966).

28. T. T. Bardin, R. C. Barrett, R. C. Cohen, S. Devons, D. Hitlin, E. Macagno, C. Nissim-Sabat, J. Rainwater, K. Runge, and C. S. Wu, Phys. Rev. Letters 16, 718 (1966).

29. A. Astbury, J. P. Deutsch, K. M. Crowe, R. E. Shafer, and R. E. Taylor, Compt. Rend. Congr. Intern. Phys. Nucl. 2, 225 (1964). See also Bull. Am. Phys. Soc. (2) 9, 393 (1964).

30. R. E. Shafer, K. M. Crowe, and D. A. Jenkins, Phys. Rev. Letters 14, 923 (1965). A more detailed article on this experiment is being prepared for publication by R. E. Shafer.

31. B. Lundquist and S. Nilsson (private communication, 1965) have proposed similar experiments at CERN.

Table I. Important parameters of the bent-crystal spectrometer.

Bent crystal:	Type	Quartz (310)
	Dimensions	20 by 20 by 0.6 cm^3
	Aperture	160 cm^2
	Focal circle diameter	764 cm (observed)
	Intrinsic resolution[a] (FWHM)	17 sec of arc
	Corresponding energy resolution (FWHM)[b]	$\Delta E = 1.6 \times 10^{-5} E^2$ keV
	Projected resolution at target (FWHM)	0.063 cm
	Depth of field	8 cm
	Maximum overall efficiency	$\sim 2.5 \times 10^{-6}$ at 50 keV
Sine-screw mechanism (with the low-energy arm):		
	Maximum measurable angle[a]	27 000 sec each side of center
	Corresponding minimum energy[c]	40 keV
	Precision presently obtainable[a]	±0.4 sec
	Corresponding energy precision[b]	$\sigma = \pm 3.8 \times 10^{-7} E^2$ keV
Collimator (low-energy design):		
	Overall dimensions	18 by 18 by 94 cm
	Plates	44 Pb alloy plates 1 mm thick
	Gaps	3 mm (tapered)
	Resolution (FWHM)	900 sec of arc
X-ray detector:	Type	NaI(Tℓ)
	Dimensions	$17 \times 17 \times 0.63$ cm^3
	PM Tubes	9 RCA 6810

[a] 1 sec ≈ 0.011 xu. [b] At 50 keV, the resolution is 40 eV (FWHM), and the obtainable precision about ±1 eV.

[c] First order both sides.

FIGURE LEGENDS

Fig. 1. Optical geometry of the 7.7-m bent-crystal spectrometer. When the Bragg conditions are satisfied, radiation from the source is partially diffracted by the bent crystal, forming a virtual image. The collimator is oriented to selectively transmit radiation from the virtual image.

Fig. 2. Top overall view of the spectrometer. Radiation shielding around the detector is not shown.

Fig. 3. Side view of the spectrometer. Radiation shielding around the detector is not shown.

Fig. 4. Crystal pivot assembly. The bent crystal, when in place, is about 20 in. above the center ball. Note that the graduated circle rotates with the bent crystal.

Fig. 5. Sine-screw mechanism.

Fig. 6. Linearity check of the lead screw. The data are the average of three runs. The error flag represents the assigned linearity, being ± 37 μin., corresponding to ± 0.004 xu for first-order diffraction from quartz (310).

Fig. 7. Crystal clamp blocks with the crystal in place. The radius of curvature is approximately 7.7m.

Fig. 8. Bent-crystal collimator. The Pb-alloy plates are stretched in two dimensions during installation to minimize bowing.

Fig. 9. First-order Bragg diffraction peak for a 0.25-mm-diam Au^{198} source. Optimum resolution is 17 sec of arc (FWHM).

Fig. 10. Calculated reflectivity of a 6-mm quartz (310) crystal. Note the effect of secondary extinction below 100 keV. The point at

412 keV is measured with an Au^{198} source.

Fig. 11. Calculated total efficiency for the 0.6-by 20- by 20 cm^3 quartz crystal when used with the present collimator. This does not include the effects of finite source width, natural linewidth, or detector efficiency.

Fig. 12. Schematic representation of the operation of the sine-screw mechanism. The positions of the Bragg diffraction peaks and the midpoint are measured in units of sine-screw turns from the mechanical center. The angles are exaggerated for illustrative purposes.

Fig. 13. Plot of $\sin\theta_B \cos\delta$ vs midpoint (see Fig. 12 for definition of terms) for diffraction of the 84-keV Yb^{170} γ ray. The error flags represent a fractional error of ± 15 ppm, corresponding to a wavelength uncertainty of ± 0.002 xu. Usually the spectrometer is operated with the midpoint within 0.5 sine-screw turns of the mechanical center so that $\cos\delta \approx 1$.

Fig. 14. Experimental arrangement. The incoming pion beam is analyzed by a scintillation-counter telescope as it stops in the region of the mesonic x-ray target. An autocollimator defines the bent-crystal centerline. The diffracted x rays are detected with a NaI(Tℓ) detector in coincidence with the counter telescope.

Fig. 15. Scintillation-counter telescope arrangement for mesonic x-ray studies. A threefold coincidence 123 together with a three-fold anticoincidence $\overline{C45}$ identifies a pion stopping in the titanium target.

Fig. 16. Typical diffraction peaks for mesonic x rays. These represent the 4F-3D transitions of calcium and titanium. An average of 2 to 3 events/h occur at the peak. The calcium and titanium data each represent more than 300 h of data-accumulation time.

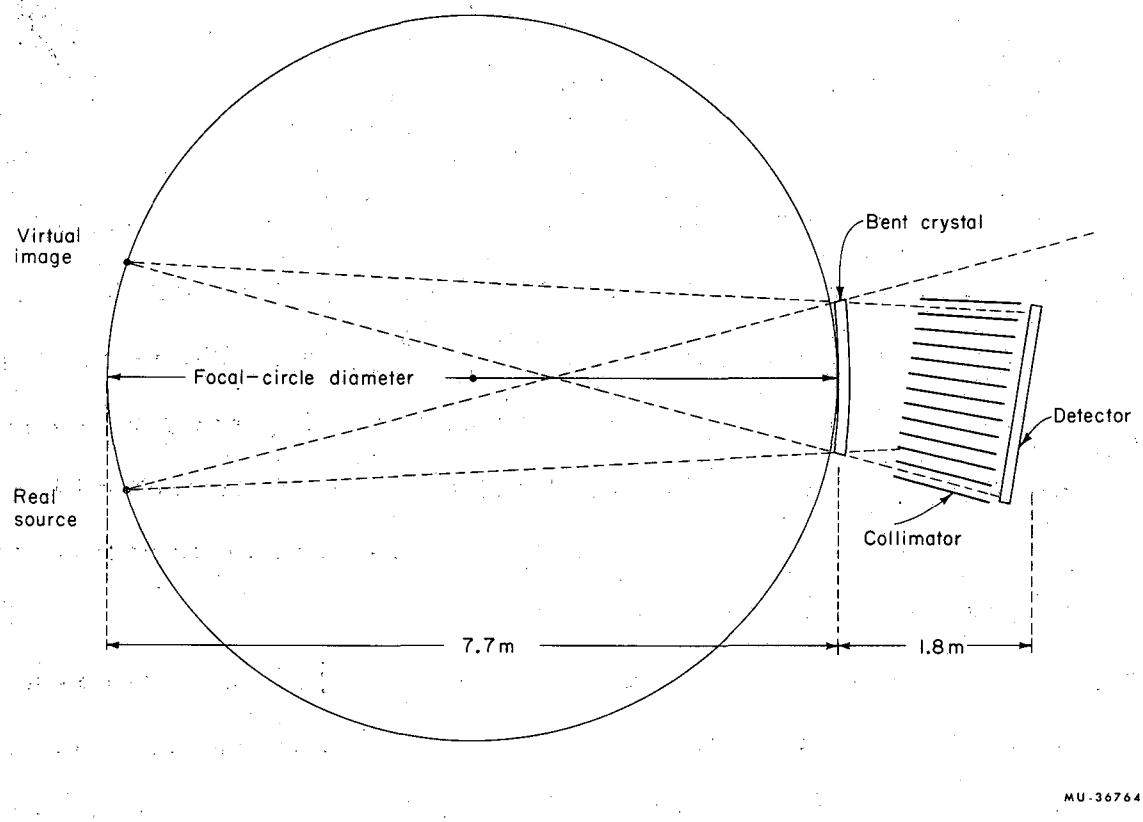
Virtual image
Bent crystal
Focal-circle diameter
Detector
Real source
Collimator
7.7 m
1.8 m
MU-36764

Fig. 1

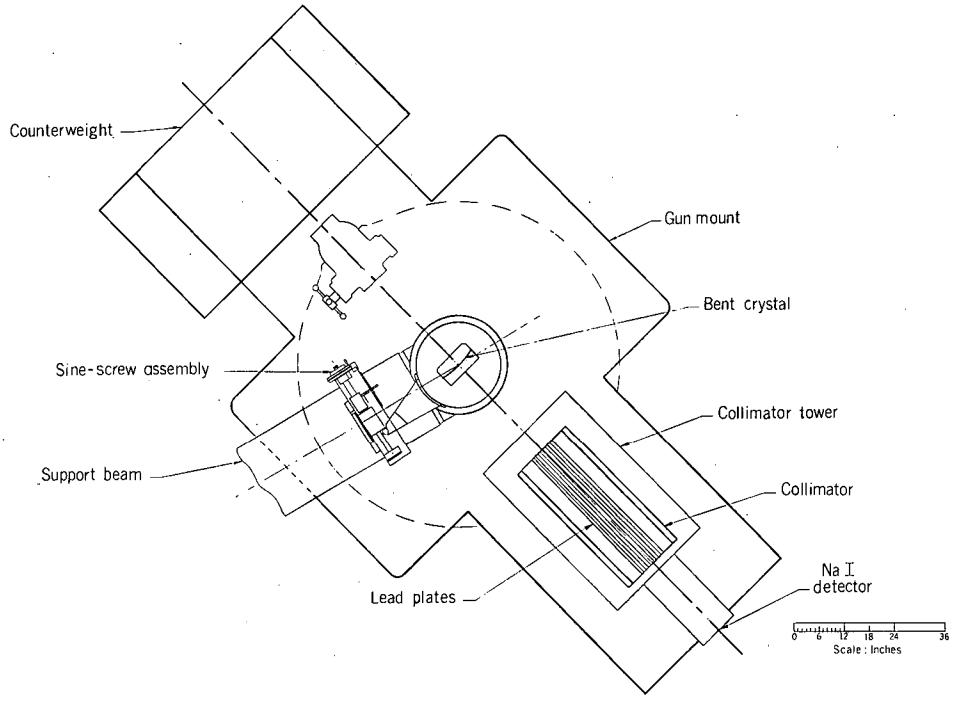

MU-36737

Fig. 2

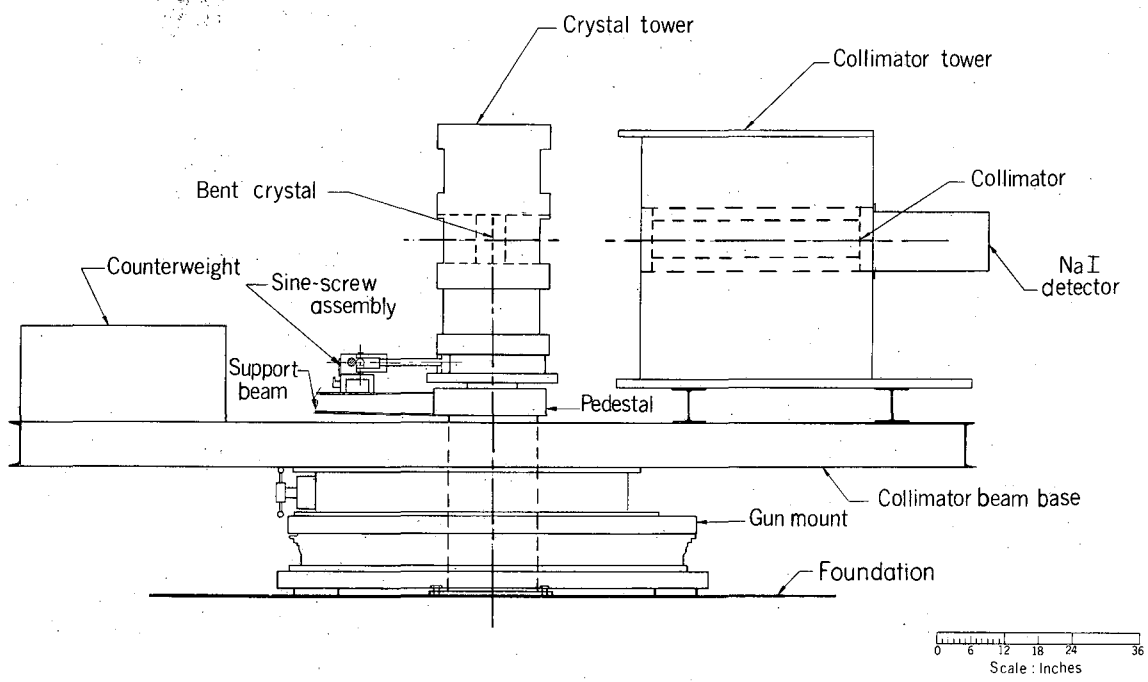

MU-36736

Fig. 3

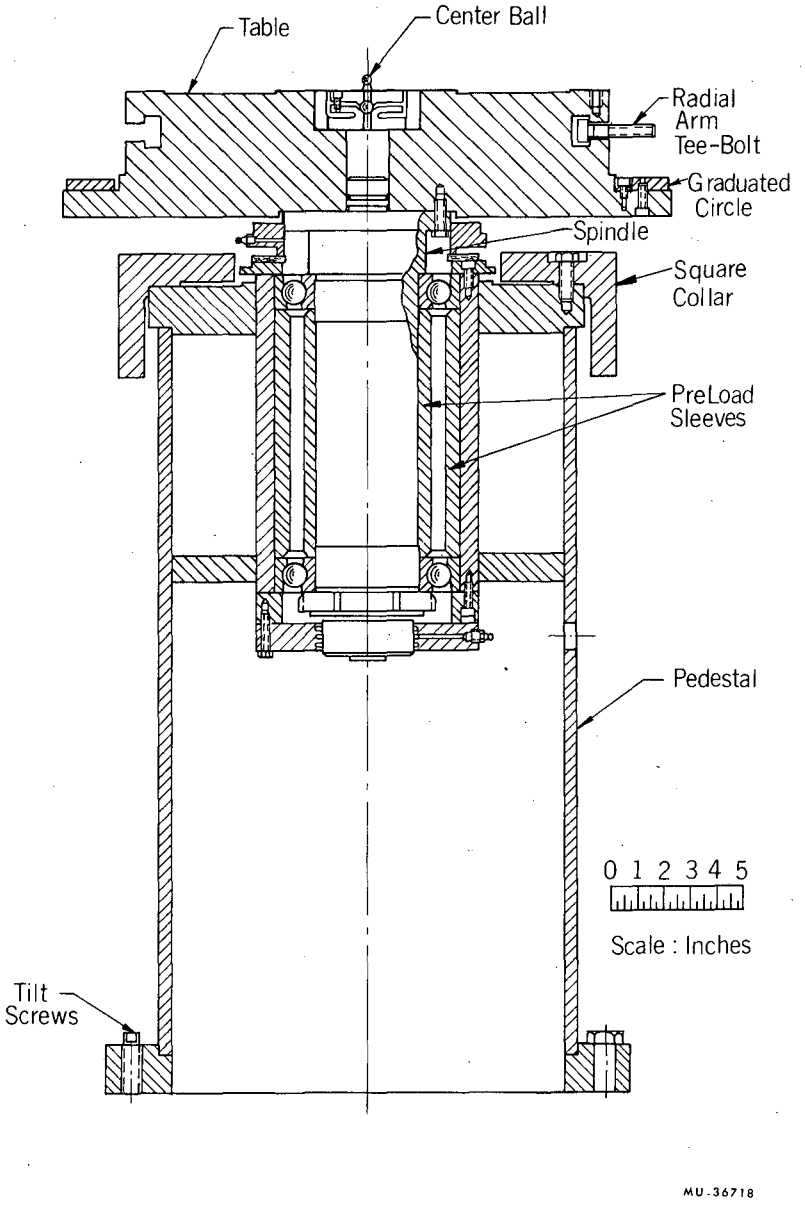
Table
Center Ball
Radial
Arm
Tee-Bolt
Graduated
Circle
Spindle
Square
Collar
PreLoad
Sleeves
Pedestal
0 1 2 3 4 5
Scale : Inches
Tilt
Screws
MU-36718

Fig. 4

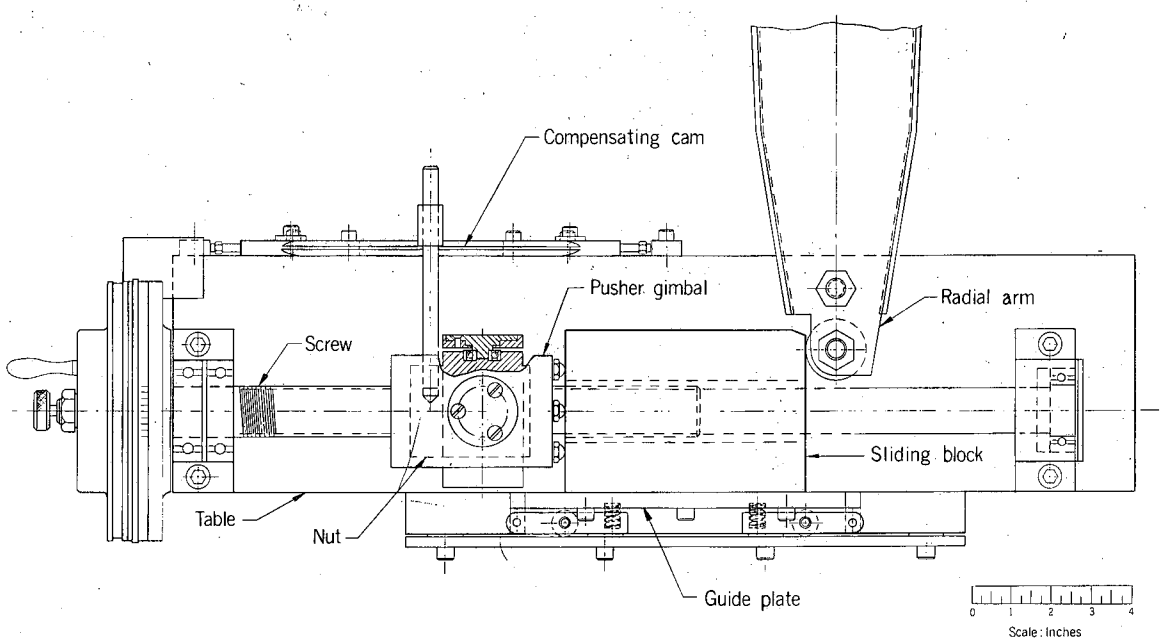

MU-36739

Fig. 5

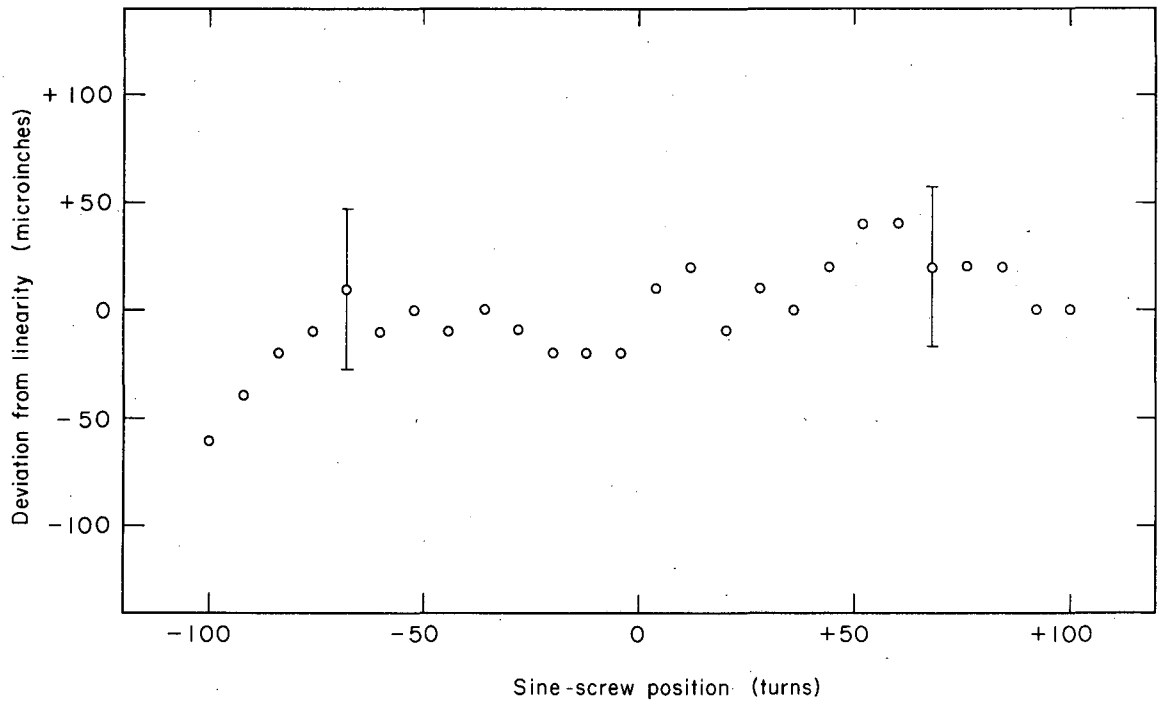

MU-36717

Fig. 6

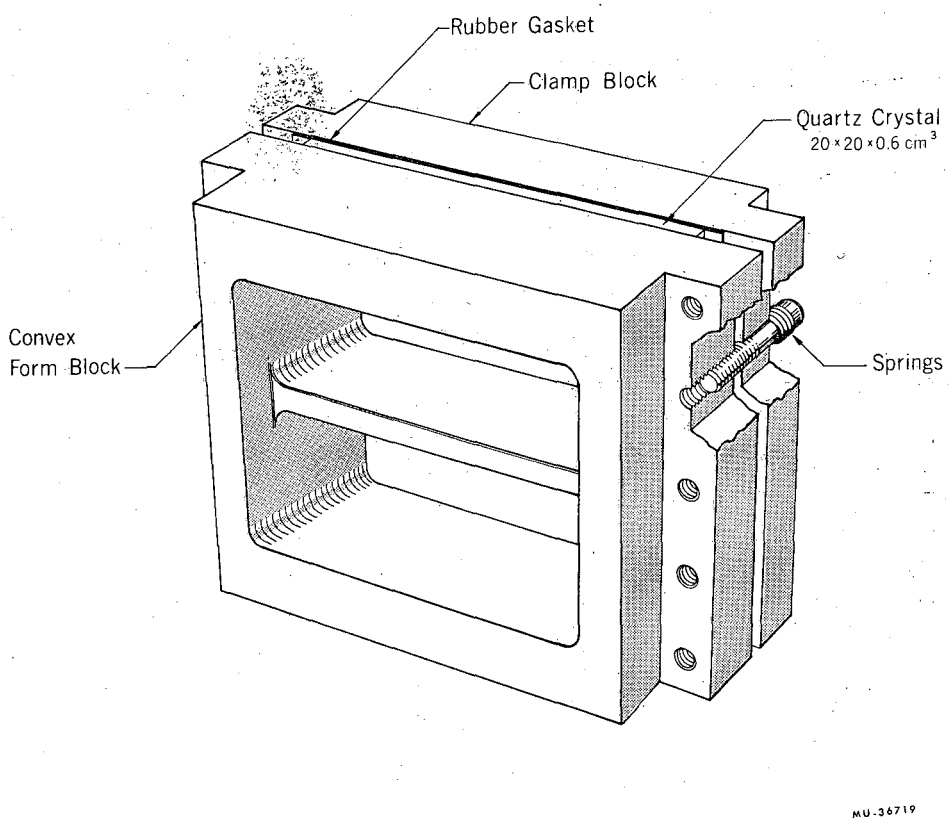
Rubber Gasket
Clamp Block
Quartz Crystal
20 × 20 × 0.6 cm³
Convex
Form Block
Springs
MU-36719

Fig. 7

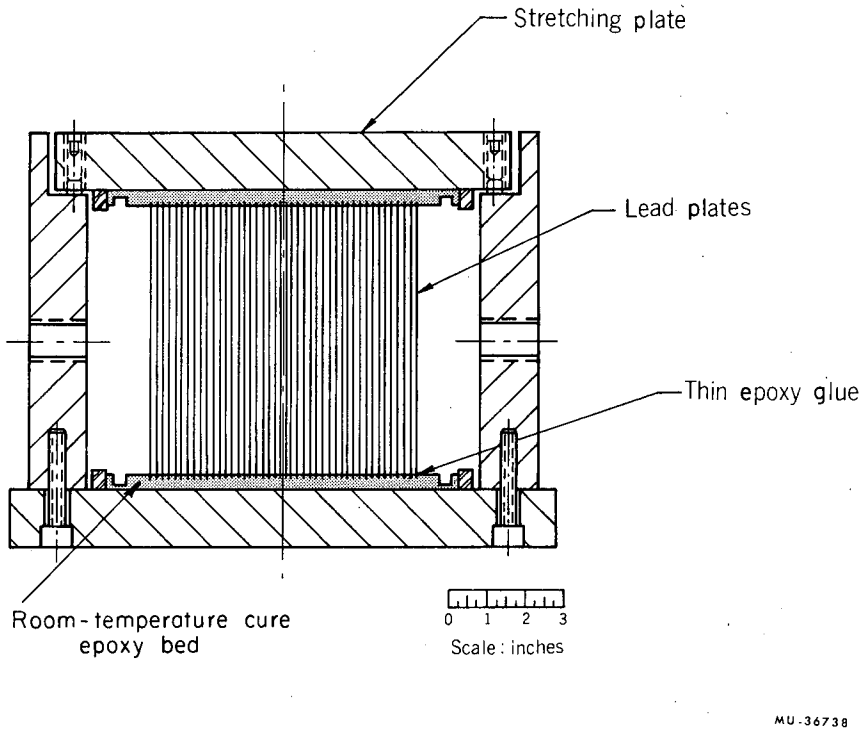
Stretching plate
Lead plates
Thin epoxy glue
Room-temperature cure epoxy bed
0 1 2 3
Scale: inches
MU-36738

Fig. 8

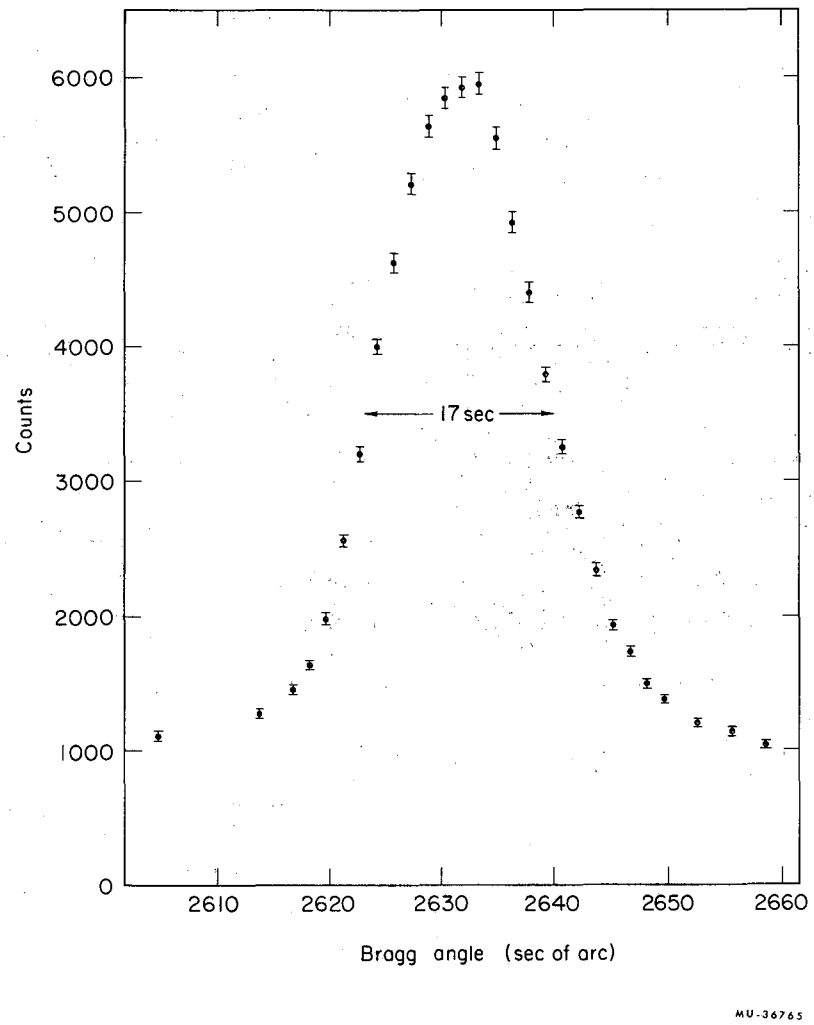
6000
5000
4000
3000
2000
1000
0
Counts
17 sec
2610
2620
2630
2640
2650
2660
Bragg angle (sec of arc)
MU-36765

Fig. 9

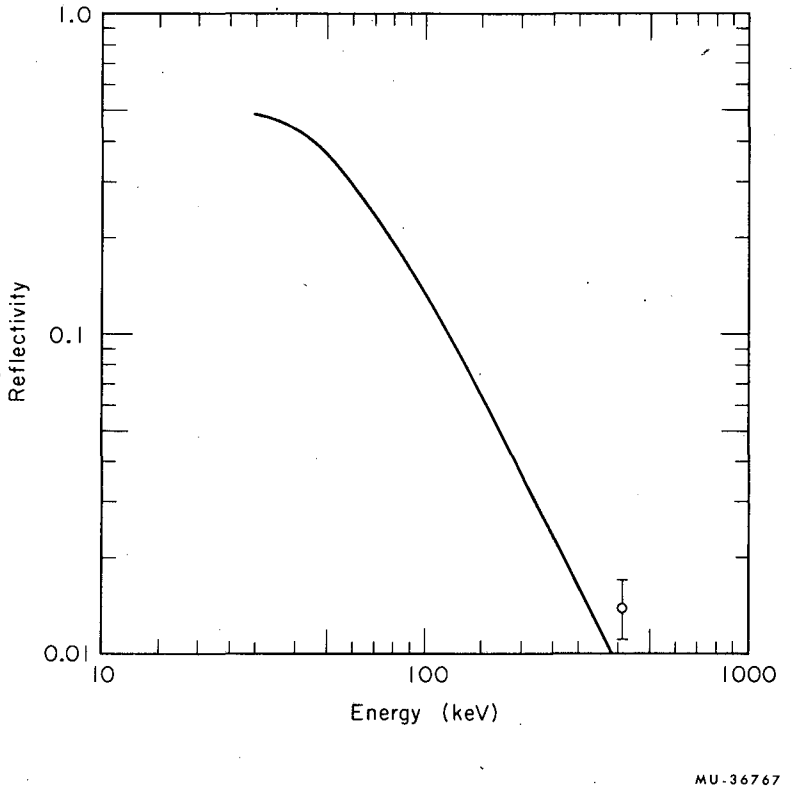

Fig. 10

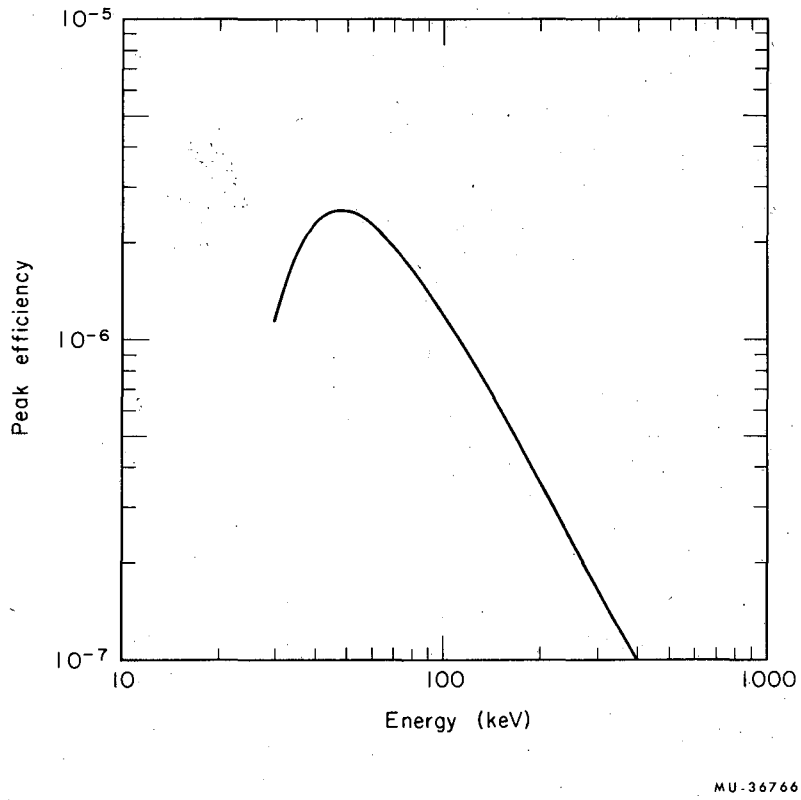

Fig. 11

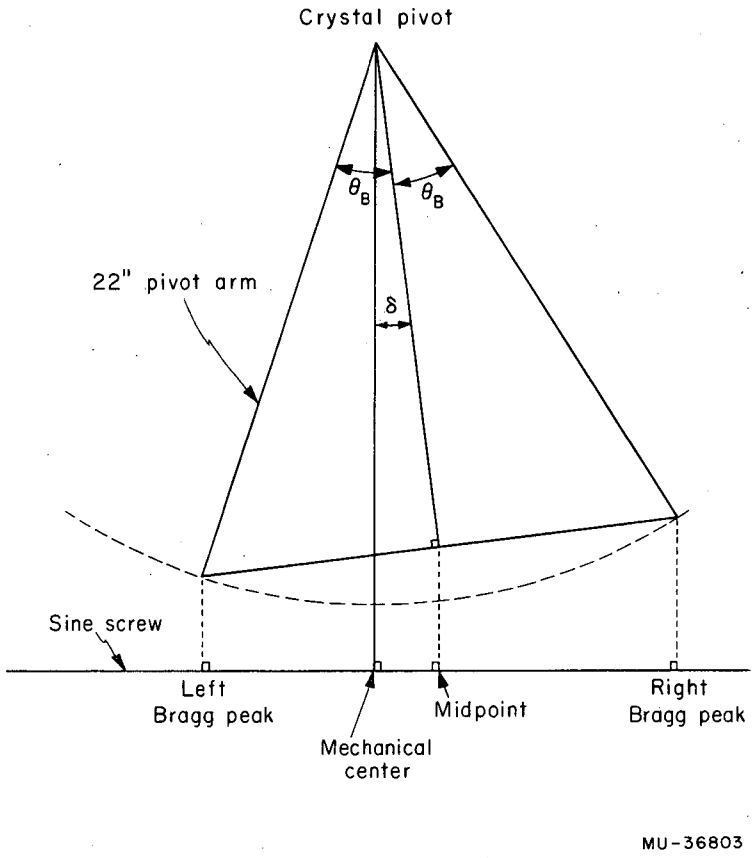
Crystal pivot
θ_B
θ_B
22" pivot arm
δ
Sine screw
Left
Bragg peak
Midpoint
Right
Bragg peak
Mechanical
center
MU-36803

Fig. 12

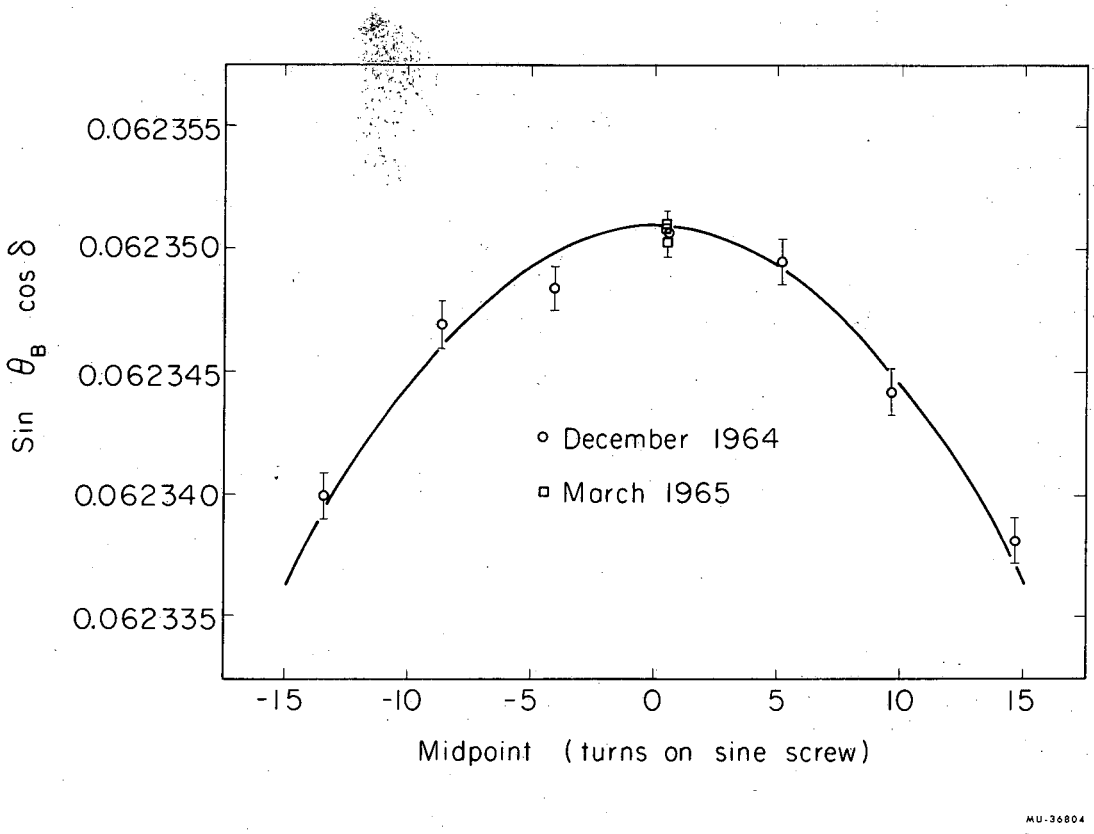
0.062355
0.062350
0.062345
0.062340
0.062335
Sin θ_B cos δ
-15
-10
-5
0
5
10
15
Midpoint (turns on sine screw)
○ December 1964
□ March 1965
MU-36804

Fig. 13

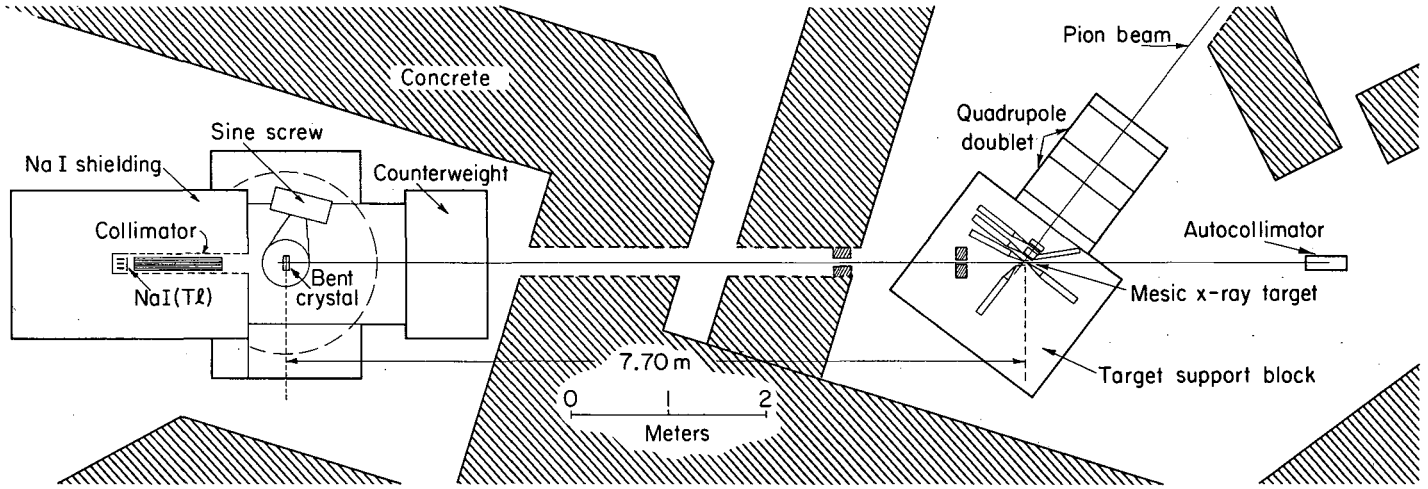
Concrete
Sine screw
Na I shielding
Counterweight
Collimator
NaI(Tℓ)
Bent crystal
7.70 m
0
1
2
Meters
Pion beam
Quadrupole doublet
Autocollimator
Mesic x-ray target
Target support block
MUB-6014

Fig. 14

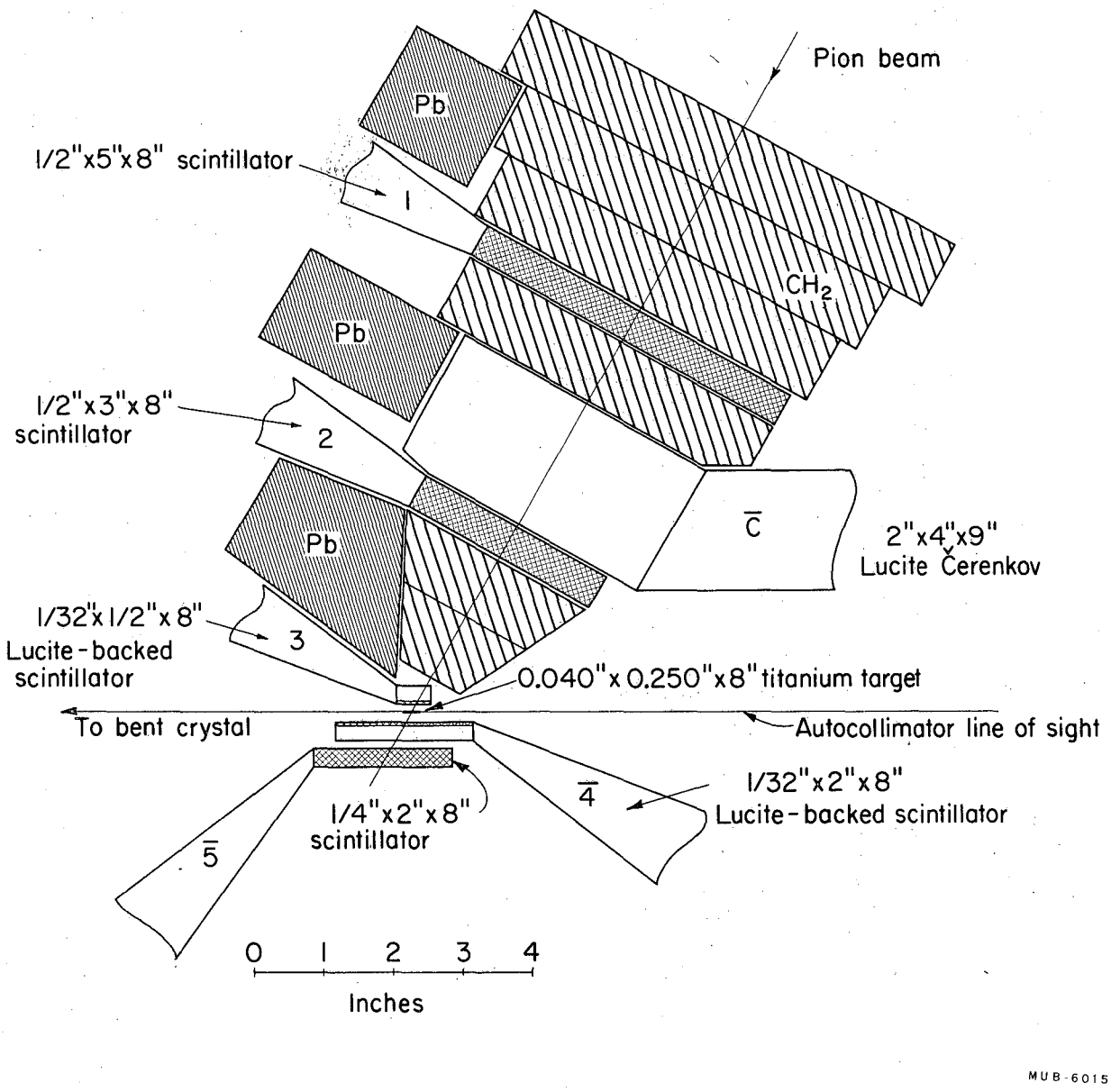
Pion beam
Pb
1/2"x5"x8" scintillator
1
CH2
Pb
1/2"x3"x8"
scintillator
2
C̄
2"x4"x9"
Lucite Čerenkov
Pb
1/32"x1/2"x8"
Lucite-backed
scintillator
3
0.040"x0.250"x8" titanium target
To bent crystal
Autocollimator line of sight
1/32"x2"x8"
Lucite-backed scintillator
4̄
1/4"x2"x8"
scintillator
5̄
0 1 2 3 4
Inches
MUB-6015

Fig. 15

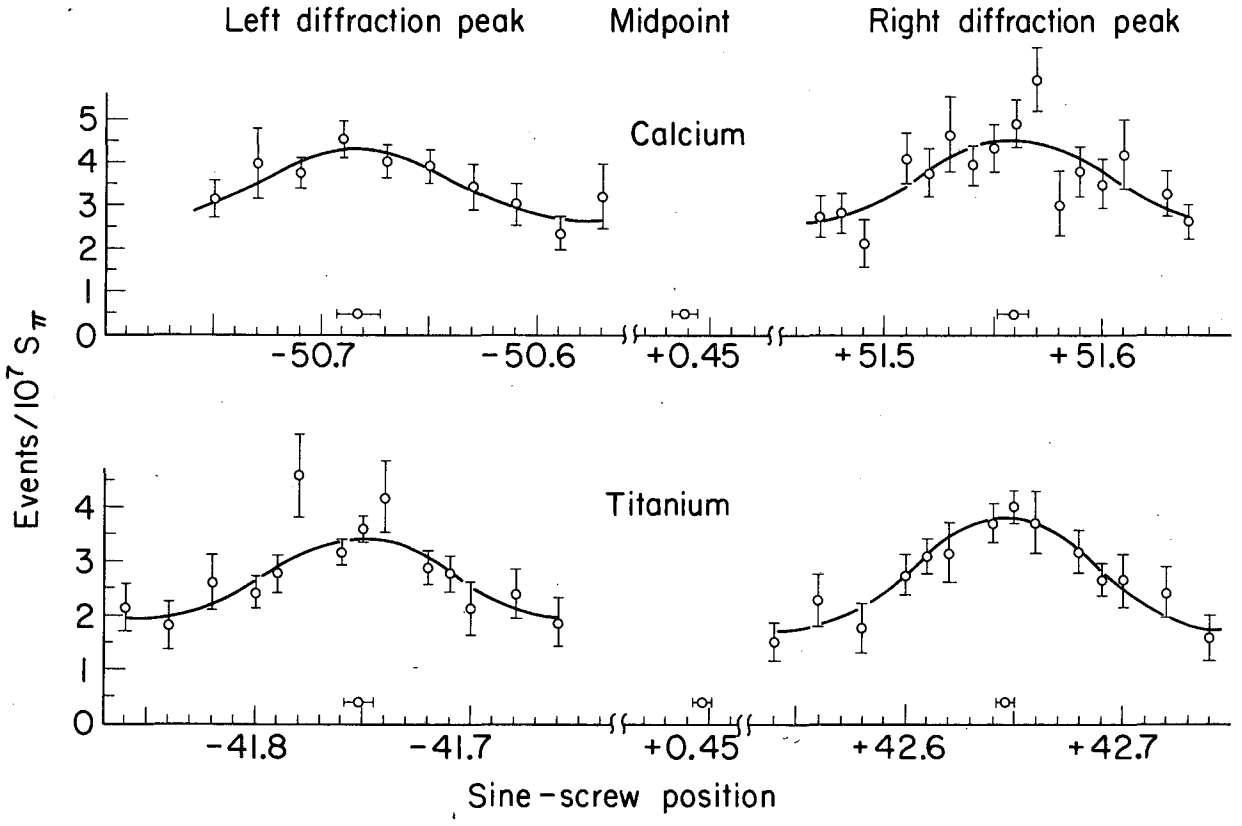

MUB-6013

Fig. 16

This report was prepared as an account of Government sponsored work. Neither the United States, nor the Commission, nor any person acting on behalf of the Commission:

A. Makes any warranty or representation, expressed or implied, with respect to the accuracy, completeness, or usefulness of the information contained in this report, or that the use of any information, apparatus, method, or process disclosed in this report may not infringe privately owned rights; or

B. Assumes any liabilities with respect to the use of, or for damages resulting from the use of any information, apparatus, method, or process disclosed in this report.

As used in the above, "person acting on behalf of the Commission" includes any employee or contractor of the Commission, or employee of such contractor, to the extent that such employee or contractor of the Commission, or employee of such contractor prepares, disseminates, or provides access to, any information pursuant to his employment or contract with the Commission, or his employment with such contractor.